Synthesis and Structural Analysis of Self-Associating Amphiphilic Statistical Copolymers in Aqueous Media

Akihito Hashidzume, Atsushi Kawaguchi, Akiyo Tagawa, Katsuhiro Hyoda, and Takahiro Sato*

Department of Macromolecular Science, Graduate School of Science, Osaka University, 1-1 Machikaneyama-cho, Toyonaka, Osaka 560-0043, Japan

Received September 6, 2005; Revised Manuscript Received December 6, 2005

ABSTRACT: Amphiphilic statistical copolymer samples of sodium 2-(acrylamido)-2-methylpropanesulfonate and *n*-hexyl methacrylate with different degrees of polymerization and compositions were prepared by reversible addition−fragmentation chain transfer copolymerization, and their self-aggregating structure in 0.1 M aqueous NaCl was studied by light scattering, fluorescence, viscometry, and size exclusion chromatography. Major components of the copolymer samples were aggregates consisting of 2−7 polymer chains and possessing 1−5 hydrophobic microdomains, depending on the degree of polymerization and composition.

Introduction

Amphiphilic polyelectrolytes comprise ionizable and hydrophobic monomer units.[1] While hydrophobic monomer units tend to associate each other by strong hydrophobic attraction in aqueous media, ionic monomer units want to separate each other as far as possible due to strong electrostatic repulsion. For diblock copolymers, the spherical micelle, the wormlike micelle, or the vesicle is formed to fulfill opposite requirements of the two types of monomer units.[2−6] On the other hand, amphiphilic statistical copolymers or hydrophobically modified polyelectrolytes[1,7] are difficult to find their conformations fulfilling both requirements, so that they may take some frustrated conformations in aqueous media. In comparison with amphiphilic block copolymers, we still know much less about conformations of amphiphilic statistical copolymers in aqueous solution, although the self-association behavior of amphiphilic statistical copolymers may be a useful model for the formation of higher-order structures of proteins.

In the present study, we have prepared statistical copolymer samples of sodium 2-(acrylamido)-2-methylpropanesulfonate (NaAMPS) and *n*-hexyl methacrylate (C_6MA) by reversible addition−fragmentation chain transfer (RAFT) polymerization[8−10] and investigated self-association structures of the copolymer samples in aqueous media by static and dynamic light scattering, steady-state and time-resolved fluorescence, viscometry, and size exclusion chromatography (SEC).

Light scattering and SEC have indicated that while the copolymer samples are dispersed molecularly in methanol solutions, they form aggregates with bimodal distributions in aqueous salt solutions. In the latter solutions, a small amount of the large aggregating component makes it difficult to characterize the major small aggregating component of the copolymer. Here we have taken advantage of the combined static and dynamic light scattering technique recently developed[11] to determine the aggregation number and hydrodynamic radius of the major small aggregate for each copolymer sample. On the other hand, time-resolved fluorescence measurements allowed us to determine the number of hydrophobic microdomains per major small aggregate.[12] These results have indicated that the major small aggregating component of the copolymer exists as unicore or multicore micelle in aqueous medium. The aggregation number and the core number were remarkably dependent on the degree of polymerization and composition.

Scheme 1. Chemical Structure of Poly(NaAMPS/C_6MA)

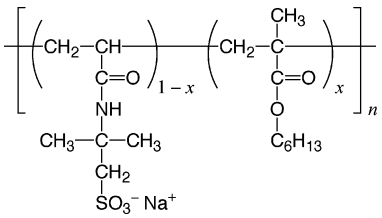

Experimental Section

Materials. C_6MA and *N*,*N*-dimethylformamide (DMF) were distilled under reduced pressure. 2,2′-Azobis(isobutyronitrile) (AIBN) (Wako Pure Chemical, Japan) was recrystallized from ethanol. 1-Cyano-1-methylethyl dithiobenzoate (CMEDTB), used as a chain transfer agent (CTA) in this study, was prepared by a slight modification of the procedure of Thang et al.[13] (see Supporting Information). Methanol was purified by atmospheric distillation. Sodium chloride (NaCl) and pyrene were recrystallized from water and ethanol, respectively. Water was purified with a Millipore Milli-Q system.

Polymer Preparation. The procedure of RAFT copolymerization of NaAMPS and C_6MA is as follows: NaAMPS and C_6MA were dissolved in DMF under an argon atmosphere using an ampule equipped with a three-way stopcock. To the monomer solution was added a DMF solution of AIBN and CTA or macro-CTA (fixing the molar ratio of (macro-)CTA relative to AIBN at 5:1), where macro-CTA is a poly(NaAMPS/C_6MA) carrying a CTA fragment prepared by RAFT copolymerization. The ampule was immersed in an oil bath thermostated at 70 °C. After 24 h, the reaction mixture was poured into a large excess of diethyl ether to precipitate polymer. The polymer obtained was purified by reprecipitation from methanol into a large excess of diethyl ether three times and dissolved in pure water. The aqueous solution was dialyzed against pure water for a week. The polymer was recovered by a freeze-drying technique.

To remove the CTA fragment from polymer chain, dithioester was hydrolyzed with Na_2CO_3. Solid polymer sample was dissolved in a solution of Na_2CO_3 in a water/methanol mixture, and then the solution was stirred overnight. The complete conversion of hydrolysis was confirmed by absorption spectroscopy. To the solution was added 1 M HCl aqueous solution to neutralization. After evaporation of the solvent, methanol was added to the residue. The solution was filtrated with a 0.45 μm PTFE membrane filter, and the filtrate was poured into a large excess of diethyl ether for reprecipitation. The polymer was dissolved in pure water, and

10.1021/ma051950d CCC: $33.50
Published on Web 01/14/2006

Table 1. Molecular Characterization of Poly(NaAMPS/C_6MA) Samples in Methanol with 0.2 M $LiClO_4$

sample	x	M_w/M_n	$M_w/10^4$	N_{0w}	$N_{0,C6}$	$A_2{}^a$	R_H/nm	$[\eta]$/cm^3 g^{-1}
$M1_{x=0.3}$	0.32	1.20	1.1	53	17	6.7_5	2.4	9.7
$M2_{x=0.3}$	0.36	1.21	2.0	95	34	7.6	3.5	11.1
$M3_{x=0.3}$	0.31	1.21	3.3	160	49	4.1	4.2	15.4
$M5_{x=0.3}$	0.30	1.23	4.9	230	70	3.1	5.8	18.8
$M4_{x=0.2}$	0.22	1.20	4.3	200	44	5.4	6.1	

[a] In units of 10^{-4} mol cm^3 g^{-2}.

aqueous solution was dialyzed against pure water for a few weeks. The polymer was recovered from the aqueous solution by a freeze-drying technique.

Preparation of Test Solutions. Copolymer samples were dissolved in pure water and in methanol at room temperature. Then the aqueous and methanol solutions were diluted with 0.2 M aqueous NaCl and methanol containing 0.4 M $LiClO_4$, respectively, by 1:1 volume ratio to adjust the ionic strength, and were used in the following measurements.

Size Exclusion Chromatography (SEC). SEC measurements were performed by using two instruments. One was a JASCO GPC-900 instrument equipped with a Shodex Asahipak GH-7M HQ column (at 40 °C) and a refractive index detector (JASCO RI-930), using methanol with 0.2 M $LiClO_4$ as the eluent. Ratios of the weight- to number-average molecular weight M_w/M_n of poly(NaAMPS/C_6MA) samples were estimated with a calibration curve of M_w against the peak elution volume for the poly(NaAMPS/C_6MA) samples, where M_w were determined by static light scattering (see below). As shown in Table 1, M_w/M_n of all samples prepared are ca. 1.2, indicating that the molecular weight distributions of the samples are considerable narrow.

The other instrument used was a Shodex HPLC equipped with a Shodex KW-804 column (at 25 °C), and the eluent was 0.1 M aqueous NaCl solution. The elution was monitored by a multiangle light scattering detector (Wyatt Technology DAWN EOS) and a refractometer (Shodex RI-71).

NMR. ^{1}H NMR spectra of the copolymers were measured with a JEOL JNM EX270 spectrometer using D_2O as a solvent at 30 °C. Contents of the C_6MA unit in the copolymer samples were determined from the ratio of area intensities of the resonance peaks due to methyl protons in the *n*-hexyl group in C_6MA and methylene protons in NaAMPS.

Light Scattering Measurements. Test solutions for light scattering measurements were optically cleaned by filtration through a 0.8 μm pore-size membrane filter, followed by a 3 h centrifugation at 5000*g*. Simultaneous static and dynamic light scattering measurements for poly(NaAMPS/C_6MA) in 0.1 M aqueous NaCl and methanol with 0.2 M $LiClO_4$ were made at 25 °C using an ALV/DLS/SLS-5000 light scattering system equipped with an ALV-5000 multiple τ digital correlator. Vertically polarized light with the wavelength λ_0 of 532 nm emitted from an Nd:YAG laser was used as the incident light, and the scattered light was measured with no analyzer. The light scattering system was calibrated using toluene as the reference material. The Rayleigh ratio R_{tol} of toluene for vertically polarized 532 nm light without analyzer was taken to be 2.72×10^{-5} cm^{-1} at 25 °C. The excess Rayleigh ratio R_θ at the scattering angle θ of each solution over that of the solvent was calculated from the scattering intensity of the solution $I_{\theta,soln}$ and solvent $I_{\theta,solv}$ by the standard procedure.[11]

The intensity autocorrelation function $g^{(2)}(t)$ obtained by dynamic light scattering was analyzed by a CONTIN program to estimate the spectrum $A(\tau,k)$ of the relaxation time τ in the logarithmic scale at each scattering angle or the magnitude of the scattering vector k: $[g^{(2)}(t) - 1]^{1/2} = [g^{(2)}(0) - 1]^{1/2} \int A(\tau,k) \exp(-t/\tau)\, d(\ln \tau)$. For all aqueous NaCl solutions, $A(\tau,k)$ was bimodal, indicating the existence of two scattering components with fast and slow relaxation times. From $A(\tau,k)$ data, R_θ obtained from static light scattering was divided into the fast- and slow-relaxation components ($R_{\theta,fast}$ and $R_{\theta,slow}$).[11]

When the solution is dilute enough, $R_{\theta,i}$ (i = fast, slow) can be written as

$$\lim_{\theta\to 0}\left(\frac{Kc}{R_{\theta,i}}\right)^{1/2} = \frac{1}{(w_i M_{w,i})^{1/2}} + A_{2,i}(w_i M_{w,i})^{1/2}\, c + ... \qquad (1)$$

and

$$\lim_{c\to 0}\left(\frac{Kc}{R_{\theta,i}}\right)^{1/2} = \frac{1}{(w_i M_{w,i})^{1/2}}\left(1 + \frac{1}{6}\langle S^2\rangle_{z,i} k^2 + ...\right) \qquad (2)$$

where K is the optical constant, c is the total polymer mass concentration, and w_i, $M_{w,i}$, $\langle S^2\rangle_{z,i}$, and $A_{2,i}$ are the weight fraction (in the total polymer), weight-average molar mass, z-average mean-square radius of gyration, and second virial coefficient of the component i, respectively. Generally speaking, eqs 1 and 2 are not necessarily applicable to copolymer samples with composition distributions, but it can be shown that the equations are good approximations for our copolymer samples.[14] If $w_{slow} \ll w_{fast}$, $A_{2,fast}$ is equal to the second virial coefficient between fast-relaxation components, while $A_{2,slow}$ approximately equals the one between the fast- and slow-relaxation components multiplied by $w_{fast}M_{w,fast}/w_{slow}M_{w,slow}$.

The first cumulants of the fast component Γ_{fast} and the slow component Γ_{slow} were estimated from bimodal $A(\tau,k)$.[11] The diffusion coefficient $D_{0,i}$ of the component i (i = fast, slow) was determined by extrapolating Γ_i/k^2 to the zero scattering angle and zero concentration and the hydrodynamic radius $R_{H,i}$ from $D_{0,i}$ using the Einstein−Stokes equation.

For methanol solutions, $A(\tau,k)$ was unimodal, so that there is only single component in methanol, and the molecular parameters M_w, A_2, and R_H in methanol were determined by the conventional analysis of static and dynamic light scattering data.

Specific Refractive Index Increment Measurements. Specific refractive index increments ($\partial n/\partial c$) were measured for dialyzed solutions of sample $M5_{x=0.3}$ dissolved in 0.1 M aqueous NaCl and in methanol with 0.2 M $LiClO_4$ at 25 °C using a Schulz-Cantow-type differential refractometer with 436 and 546 nm wavelength light. Values of $\partial n/\partial c$ at 532 nm at 25 °C were obtained by interpolation of $\partial n/\partial c$ values at 436 and 546 nm to be 0.147 cm^3/g in 0.1 M aqueous NaCl and 0.153 cm^3/g in methanol with 0.2 M $LiClO_4$.

Viscosity Measurements. Viscosities of poly(NaAMPS/C_6MA) in 0.1 M aqueous NaCl and in methanol with 0.2 M $LiClO_4$ were measured at 25 °C using conventional capillary viscometers of the Ubbelohde type. The intrinsic viscosity $[\eta]$ and the Huggins coefficient k' were determined using the Huggins and Mead−Fuoss plots.

Fluorescence Measurements. A small amount of methanol solution containing pyrene (ca. 1 wt %) was added to 0.1 M aqueous NaCl solutions of poly(NaAMPS/C_6MA) samples under vigorous stirring. Then the solutions were filtrated through 0.8 μm pore-size membrane filters and used for steady-state and time-resolved fluorescence measurements. The concentration of solubilized pyrene was determined by absorption spectroscopy.

Steady-state fluorescence spectra were recorded on a Hitachi F-4500 fluorescence spectrometer. Emission spectra of pyrene were measured with excitation at 337 nm at room temperature. The slit widths for excitation side were kept at 2.5 nm during measurement.

Fluorescence decay data were collected on a HORIBA NAES 550 system equipped with a flash lamp filled with hydrogen. The solution containing pyrene probe was excited at 337 nm, and pyrene fluorescence was monitored around 400 nm with a band-pass filter (Toshiba KL-40) and a cutoff filter (Toshiba L-37) placed between the sample and detector. Test solutions were purged with argon for about 30 min prior to measurements.

The fluorescence decay curves were analyzed on the basis of the Inferta−Tachiya kinetics[12,15−18] for the fluorescence quenching experiment where fluorophores and quenchers are solubilized in the solution:

$$\ln[I(t)/I(0)] = -k_0' t - \bar{n}'[1 - \exp(-k_E' t)] \quad (3)$$

with k_0', $\bar{n}$, and k_E', defined by

$$k_0' \equiv k_0 + \frac{k_E k_-}{k_E + k_-}\bar{n}, \quad \bar{n}' \equiv \left(\frac{k_E}{k_E + k_-}\right)^2 \bar{n}, \quad k_E' \equiv k_E + k_- \quad (4)$$

Here, k_0 is the fluorescence decay rate constant for the excited probe in the absence of quenchers, k_E is the pseudo-first-order rate constant for quenching in a micelle containing one quencher, k_- is the first-order rate constant for exit of a given probe molecule from a micelle, and $\bar{n}$ is the average number of quenchers contained in a micelle.

For our pyrene excimer formation experiment, pyrene molecules act as both fluorophore and quencher, and the corresponding kinetic equation is slightly different from that for the Infelta−Tachiya model. However, the final equation for the fluorescence decay has the same form as eq 3 along with eq 4. The difference is meanings of the parameters k_E, k_-, and $\bar{n}$ in eq 4; $\bar{n}$ is the average number of total pyrene molecules (acting as both fluorophore and quencher) in a micelle, instead of the average quencher number in the Infelta−Tachiya equation, while k_E and k_- are the rate constants for the excimer formation in a micelle containing two pyrene molecules and for exit of a free pyrene molecule from the micelle, respectively.

Results

In Methanol with 0.2 M $LiClO_4$. Figure 1a shows the angular dependence of $(Kc/R_\theta)^{1/2}$ for sample $M5_{x=0.3}$ in methanol with 0.2 M $LiClO_4$ at 25 °C. We have determined $(Kc/R_0)^{1/2}$ from the intercepts of the lines shown. The dynamic light scattering result for the same sample ($c = 0.011$ g/cm^3; $\theta = 45°$) is shown in panel b of Figure 1. The relaxation time spectrum $A(\tau,k)$ obtained from the intensity autocorrelation function $g^{(2)}(t)$ has a single peak. The first cumulant Γ was calculated from $A(\tau,k)$.[11] Although not shown, Γ/k^2 obtained for different θ was almost independent of k^2. Figure 2 shows concentration dependencies of $(Kc/R_0)^{1/2}$ and Γ/k^2 for all samples measured in methanol with 0.2 M $LiClO_4$. We have determined the weight-average molecular weight M_w, the second virial coefficient A_2, and the hydrodynamic radius R_H, from the two plots. Table 1 lists the results as well as the weight-average degree of polymerization N_{0w} calculated from M_w and the average molar mass $\bar{M}_0$ per monomer unit and the number $N_{0,C6}$ ($= xN_{0w}$) of hydrophobic monomer units per chain. The values of A_2 indicate that methanol solution with 0.2 M $LiClO_4$ is a good solvent for poly(NaAMPS/C_6MA). Table 1 also contains results of viscometry for methanol solutions of four samples with $x \sim 0.3$.

Figure 3 plots $[\eta]$ (filled squares) for poly(NaAMPS/C_6MA) with $x \sim 0.3$ in methanol with 0.2 M $LiClO_4$ against the weight-average degree of polymerization N_{0w} and compares them with recent Hagino et al.'s $[\eta]$ data for NaAMPS homopolymer[19] [poly(NaAMPS)] in 0.5 M aqueous NaCl at 25 °C (unfilled squares), where $[\eta]$ is multiplied by the monomer-unit molar mass ratio of poly(NaAMPS) to poly(NaAMPS/C_6MA) with $x \sim 0.3$ ($= 229/210$). Here, it is noted that the Debye screening length in methanol with 0.2 M $LiClO_4$ is almost equal to that in 0.5 M aqueous NaCl. Our copolymer results almost agree with the poly(NaAMPS) data.

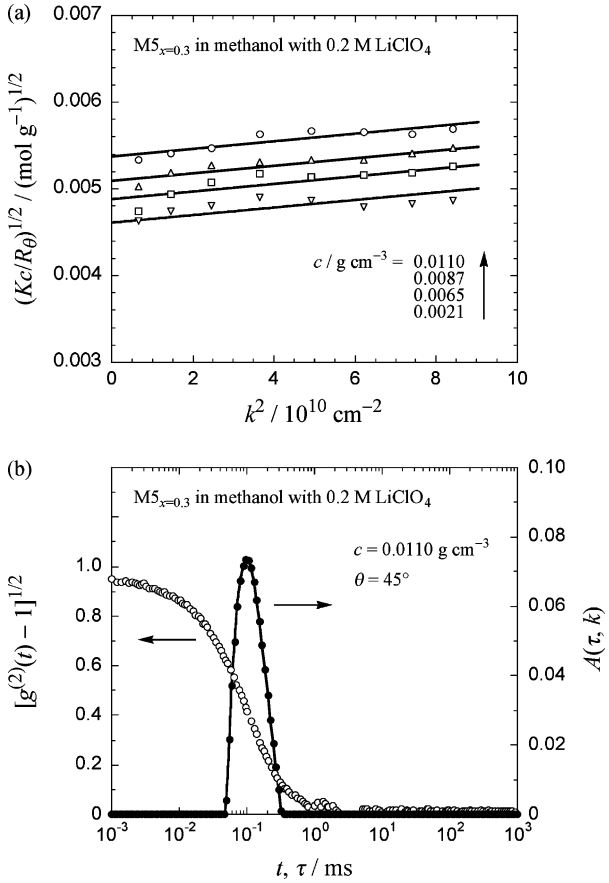

Figure 1. (a) Static and (b) dynamic light scattering results for sample $M5_{x=0.3}$ in methanol with 0.2 M $LiClO_4$ at 25 °C.

Figure 3 also shows the relation between R_H (filled circles and a triangle) and N_{0w} for poly(NaAMPS/C_6MA) with $x \sim 0.3$ and 0.2 in methanol with 0.2 M $LiClO_4$. The relation is almost independent of x in this solvent and essentially agrees with the relation for the NaAMPS homopolymer in 0.5 M aqueous NaCl at 25 °C, which was recently obtained by Yashiro et al.[20]

In 0.1 M Aqueous NaCl. Figure 4 shows static and dynamic light scattering results for sample $M3_{x=0.3}$ in 0.1 M aqueous NaCl. The static light scattering exhibits a strong angular dependence (panel a), and dynamic light scattering shows bimodal relaxation (panel b). These results indicate that the aqueous solution contains two scattering components with largely different sizes. Using $A(\tau,k)$ data for different k, we have separated the static light scattering results into fast- and slow-relaxation components, which are shown in panels a and b of Figure 5, respectively. The k^2 dependence of $(Kc/R_\theta)_{fast}^{1/2}$ is weak, and that of $(Kc/R_\theta)_{slow}^{1/2}$ is strong. Similar results were obtained for other poly(NaAMPS/C_6MA) samples.

Zero-angle values $(Kc/R_0)_{fast}^{1/2}$ were obtained from intercepts of the lines indicated in Figure 5a. The results are plotted against c in Figure 6a along with other sample data. From intercepts and slopes of the plots, we have estimated $w_{fast}M_{w,fast}$ and $A_{2,fast}$ using eq 1. On the other hand, the first cumulant Γ_{fast} of the fast-relaxation component was calculated from $A(\tau,k)$ as a function of k, and Γ_{fast}/k^2 was extrapolated to zero k. Figure 6b plots extrapolated Γ_{fast}/k^2 against c for all samples investigated.[21] The diffusion coefficient was determined from the intercept of each plot, and the hydrodynamic radius $R_{H,fast}$ of the fast-

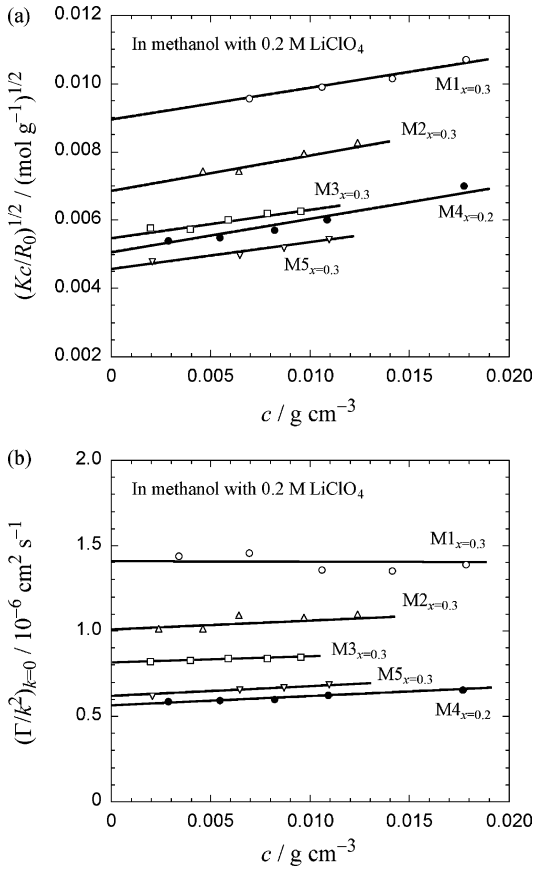

Figure 2. Concentration dependencies of $(Kc/R_0)^{1/2}$ and $(\Gamma/k^2)_{k=0}$ for all poly(NaAMPS/C_6MA) samples measured in methanol with 0.2 M $LiClO_4$.

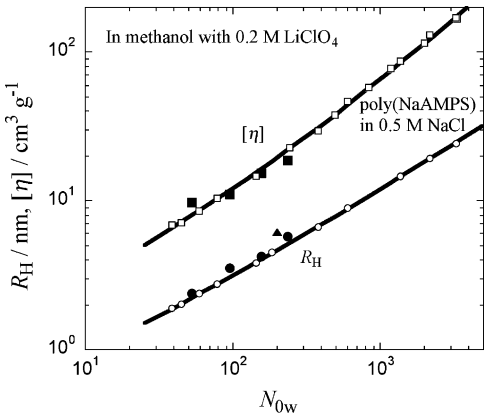

Figure 3. Plots of R_H (filled circles for $x = 0.3$ and a filled triangle for $x = 0.2$) and $[\eta]$ (filled squares for $x = 0.3$) against N_{0w} for poly(NaAMPS/C_6MA) samples in methanol with 0.2 M $LiClO_4$; unfilled circles and squares, corresponding N_{0w} dependencies of R_H and $[\eta]$, respectively, for NaAMPS homopolymer in 0.5 M aqueous NaCl obtained by Yashiro et al.[20] and Hagino et al.,[19] respectively.

relaxation component was calculated from the diffusion coefficient. All results are listed in Table 2.

The slow-relaxation component of poly(NaAMPS/C_6MA) in 0.1 M aqueous NaCl was analyzed in a similar way. Table 3 summarizes the results. It is noted that the k dependence of $(Kc/R_\theta)_{slow}^{1/2}$ was strong enough to estimate the radius of gyration $\langle S^2\rangle_{z,slow}^{1/2}$ using eq 2 (cf. Figure 5b), but the concentration dependence of $(Kc/R_0)_{slow}^{1/2}$ was too weak to estimate $A_{2,slow}$. Ratios ρ of $\langle S^2\rangle_{z,slow}^{1/2}$ to $R_{H,slow}$ are around unity, indicating that the slow-relaxation component of poly(NaAMPS/C_6MA) in aqueous NaCl is a physically cross-linked microgel with a low cross-link density. The information on the aggregate is,

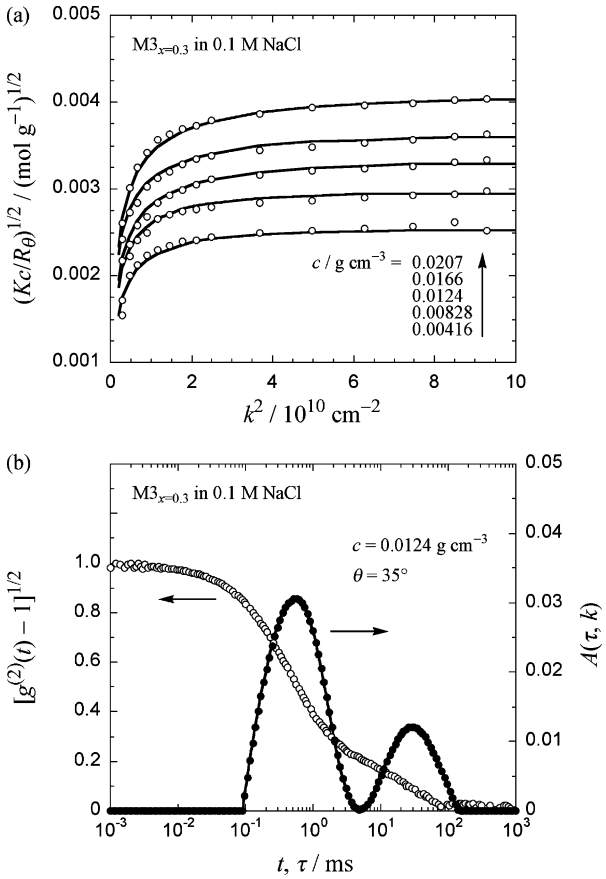

Figure 4. (a) Static and (b) dynamic light scattering results for sample $M3_{x=0.3}$ in 0.1 M aqueous NaCl.

however, not enough to argue its detailed network structure as well as the origin of physical cross-linking. It is noted that the slow mode relaxation observed in poly(NaAMPS/C_6MA) solutions has nothing to do with the "polyelectrolyte effect" reported frequently in the polyelectrolyte literature because 0.05 and 0.5 M aqueous NaCl solutions of NaAMPS homopolymer showed no slow mode relaxations in dynamic light scattering.[20] Hydrophobic monomer units must play some roles in the formation of the large aggregate in the copolymer solutions.

Although we cannot determine the molar mass $M_{w,slow}$ of the large aggregate from light scattering results alone, we can estimate the lower limit of $M_{w,slow}$ from $R_{H,slow}$. Because of the branching architecture and hydrophobic interaction of the large aggregate, $R_{H,slow}$ should be less than R_H of the NaAMPS homopolymer with the degree of polymerization equal to $M_{w,slow}/\bar{M}_0$. Though R_H of poly(NaAMPS) in 0.1 M aqueous NaCl has not been reported yet, we can estimate R_H from $[\eta]$ data in 0.1 M aqueous NaCl recently measured by Hagino et al.[19,22] using the relation $R_H = (3[\eta]M_w/4\pi N_A\varphi)^{1/3}$ (N_A: the Avogadro constant) with the universal constant $\varphi = 3.2$ (the average value estimated from Yashiro et al.'s R_H and $[\eta]$ data of poly(NaAMPS) in 0.05 and 0.5 M aqueous NaCl[20]). By extrapolating the R_H results such obtained to higher N_{0w}, we can estimate N_{0w} of NaAMPS homopolymer with $R_H = R_{H,slow}$, which is the lower limit of $M_{w,slow}/\bar{M}_0$ of the poly(NaAMPS/C_6MA) large aggregate. Table 3 lists the results of the lower limit of $M_{w,slow}$. From these $M_{w,slow}$, it turns out that w_{slow} does not exceed 0.015 for all poly(NaAMPS/C_6MA) samples, and the fast-relaxation component is the majority in 0.1 M aqueous NaCl.

Since $w_{slow} \ll 1$, we can approximate $w_{fast}M_{w,fast}$ to $M_{w,fast}$, and Table 2 lists the aggregation number $M_{w,fast}/M_w$ of the fast-

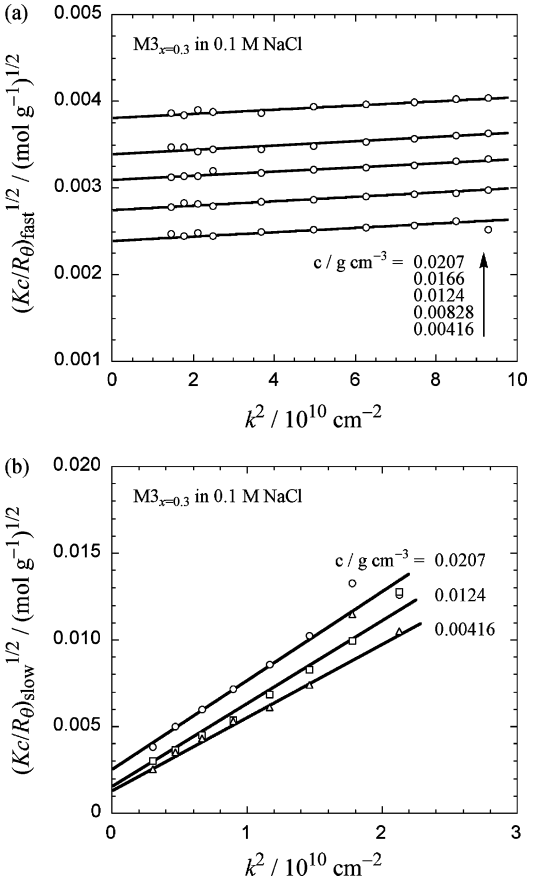

Figure 5. Angular dependencies of (a) fast- and (b) slow-relaxation components of $(Kc/R_\theta)^{1/2}$ obtained from the data shown in Figure 4a and $A(\tau,k)$.

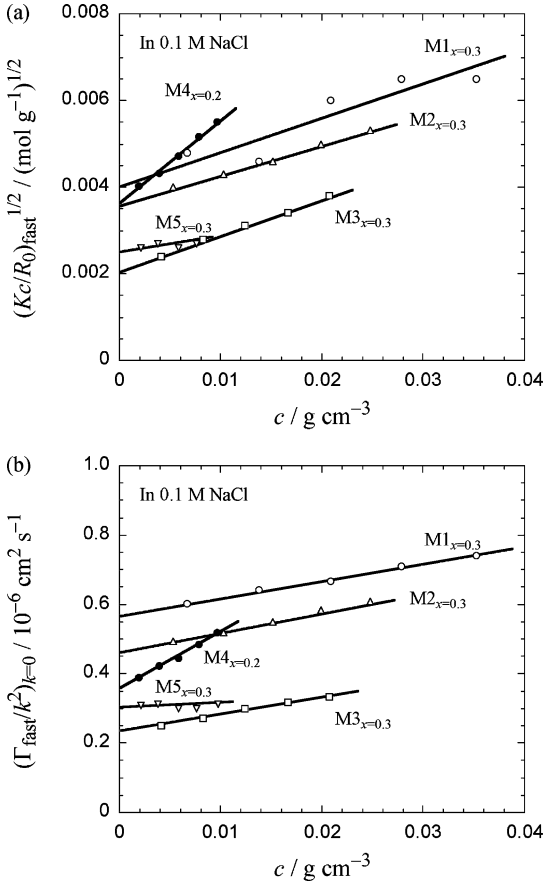

Figure 6. Concentration dependencies of (a) $(Kc/R_0)_{fast}^{1/2}$ and (b) $(\Gamma_{fast}/k^2)_{k=0}$ for five poly(NaAMPS/C_6MA) samples in 0.1 M aqueous NaCl.

relaxation component in 0.1 M aqueous NaCl, where M_w is the molecular weight of each sample determined in methanol with 0.2 M $LiClO_4$. While $M_{w,fast}/M_w$ seems to reduce with decreasing x at same N_{0w}, it does not exhibit a monotonic N_{0w} dependence. At present, we have no explanation of the large aggregation number of sample $M3_{x=0.3}$.

Figure 7 plots $R_{H,fast}$ against $N_{0w,fast} = M_{w,fast}/\bar{M}_0$ for poly(NaAMPS/C_6MA) with $x \sim 0.3$ (unfilled circles) and 0.2 (an unfilled triangle). All data points are below the line of R_H vs N_{0w} for NaAMPS homopolymer in 0.1 M aqueous NaCl indicated by the solid line in the same figure, which is drawn from Hagino et al.'s $[\eta]$ data[19] (see above). This indicates that the major small aggregate of poly(NaAMPS/C_6MA) takes a more compact conformation than the NaAMPS homopolymer does in aqueous NaCl presumably because of the hydrophobic interaction among C_6MA monomer units within the aggregate.

On the other hand, the polymer volume fraction ϕ_{in} inside the small aggregate may be approximately calculated by

$$\phi_{in} = \frac{\bar{v}M_{w,fast}/N_A}{(4\pi/3)R_{H,fast}{}^3}$$

where $\bar{v}$ is the polymer specific volume (= 0.74 cm^3/g) and N_A is the Avogadro constant. The results calculated from experimental $M_{w,fast}$ and $R_{H,fast}$ are less than 20%, as shown in the last column of Table 2. Since ϕ_{in} for globular proteins ranges from 40% to 60%,[23] the small aggregates of poly(NaAMPS/C_6MA) are not as compact as globular proteins in aqueous salt solution. We will discuss in more detail the conformation of the small aggregate (see below for filled symbols in Figure 7).

Table 2. Characterization of the Fast-Relaxation Component of Poly(NaAMPS/C_6MA) in Aqueous NaCl

sample	$w_{fast}M_{w,fast}/10^4$	$A_{2,fast}$[a]	$M_{w,fast}/M_w$[b]	$R_{H,fast}$/nm	ϕ_{in}[c]
$M1_{x=0.3}$	5.9_5	3.0	5.4	4.6	0.18
$M2_{x=0.3}$	7.7	2.4	3.9	5.9	0.11
$M3_{x=0.3}$	23	1.7	7.0	11	0.051
$M5_{x=0.3}$	15	0.27	3.0	7.7	0.096
$M4_{x=0.2}$	7.7	7.0	1.8	6.8	0.072

[a] In units of 10^{-4} cm^3 mol/g^2. [b] Assuming $w_{fast} = 1$. [c] Polymer volume fraction inside the aggregate calculated by $\phi_{in} = 3\bar{v}M_{w,fast}/4\pi N_A R_{H,fast}{}^3$ with assuming $w_{fast} = 1$ ($\bar{v}$: polymer specific volume; N_A: the Avogadro constant).

Results of Size Exclusion Chromatography (SEC). We have investigated the dispersion state of poly(NaAMPS/C_6MA) in 0.1 M aqueous NaCl also by SEC monitored by a multiangle light scattering detector and a differential refractometer. Figure 8a shows chromatograms for sample $M4_{x=0.2}$. The chromatogram I_{90} obtained by the light scattering detector at the scattering angle 90° has two peaks corresponding to $A(\tau,k)$, ascribable to the large and small elution volume peaks to the fast- and slow-relaxation components, respectively. (The very sharp peak at the smaller elution volume arises from the exclusion limit of the SEC column used.) On the other hand, the chromatogram Δn obtained by refractometry consists of a single main peak, which corresponds to the fast-relaxation component, and a very weak shoulder at the elution volume where I_{90} indicates the existence of the large aggregate. From the area ratio between the main peak and weak shoulder divided by the broken segment in the figure, we have estimated w_{slow} to be 0.006, which confirms the small w_{slow} estimated above from $R_{H,slow}$ (cf. Table 3).

Table 3. Characterization of the Slow-Relaxation Component of Poly(NaAMPS/C_6MA) in Aqueous NaCl

sample	$w_{slow}M_{w,slow}/10^5$	$\langle S^2\rangle_{z,slow}^{1/2}$/nm	$R_{H,slow}$/nm	ρ	$M_{w,slow}/10^7$	w_{slow}
$M1_{x=0.3}$	1.1	200	200	1.0	>1.5	<0.007
$M2_{x=0.3}$	2.9	220	240	0.9	>2.0	<0.015
$M3_{x=0.3}$	6.9	400	490	0.8	>6.0	<0.012
$M5_{x=0.3}$	2.5	350	270	1.3	>2.4	<0.011
$M4_{x=0.2}$	0.17	90	80	1.1	>0.35	<0.005

Using the zero-angle intensity obtained by the multiangle light scattering detector, we have calculated the weight-average molar mass M_w as a function of the elution volume, neglecting the virial terms. As shown by circles in Figure 8a, the results are also consistent with the above results of $M_{w,fast}$ and $M_{w,slow}$ obtained from batch measurements for $M4_{x=0.2}$ (cf. Tables 2 and 3).

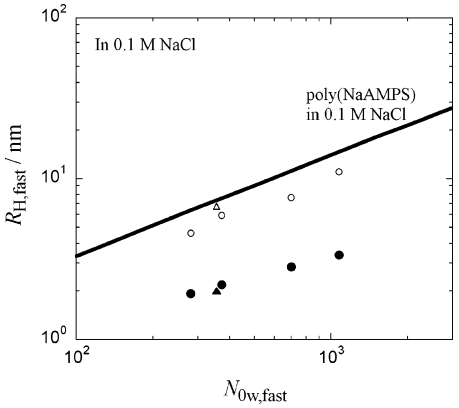

Figure 7. Plots of $R_{H,fast}$ against $N_{0w,fast}$ for poly(NaAMPS/C_6MA) with $x \sim 0.3$ (unfilled circles) and 0.2 (an unfilled triangle); solid line, the N_{0w} dependence of R_H for NaAMPS homopolymer in 0.1 M aqueous NaCl calculated from Hagino et al.'s [η] data[19] (see text); filled circles ($x \sim 0.3$) and a filled triangle ($x \sim 0.2$), maximum values of $R_{H,fast}$ estimated on the assumption that all *n*-hexyl groups of poly(NaAMPS/C_6MA) are included in the hydrophobic core(s) (see text).

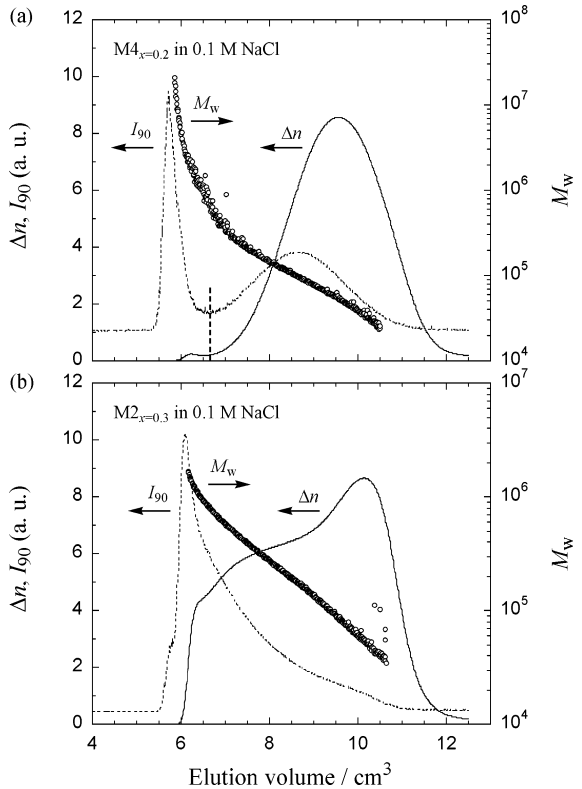

Figure 8. Size exclusion chromatograms of (a) sample $M4_{x=0.2}$ and (b) sample $M2_{x=0.3}$ in 0.1 M aqueous NaCl; solid and dotted lines and circles, chromatograms of the refractive index, light scattering intensity (at 90°), and weight-average molecular weight, respectively.

In a contrast with Figure 8a, the SEC result for sample $M2_{x=0.3}$ shown in Figure 8b is not consistent with the result of the batch measurement of light scattering. Although the chromatogram of Δn has a peak around $M_w \sim M_{w,fast}$ ($= 7.7 \times 10^4$), it is followed by a large and broad shoulder around an elution volume of 7 cm^3. Furthermore, the chromatogram of I_{90} does not resemble $A(\tau,k)$, though we can observe a weak shoulder around $M_w \sim M_{w,fast}$. These chromatograms may be due to further aggregation of small aggregates of sample $M2_{x=0.3}$ in the SEC column.

Number of Hydrophobic Microdomains per Small Aggregate. Figure 9a shows an example of fluorescence spectra of pyrene solubilized in 0.1 M aqueous NaCl solutions of sample $M5_{x=0.3}$ ($c = 5 \times 10^{-3}$ g/cm^3). The ratio I_3/I_1 of the third (383 nm) to first (372 nm) peak intensities for the solution is ca. 0.9, which is much larger than the corresponding ratio ($= 0.63$) in water[24] and comparable to that ($= 0.96$) in aqueous micellar solution of sodium dodecyl sulfate (SDS).[25] Furthermore, the concentration of pyrene solubilized in the poly(NaAMPS/C_6MA) solution highly exceeds the limiting solubility of pyrene in water (<1 μM). These results indicate that most of pyrene molecules in the copolymer solution are incorporated into hydrophobic microdomains formed by the copolymer. On the other hand, it is also indicated that plural pyrene molecules are incorporated into a hydrophobic microdomain because an

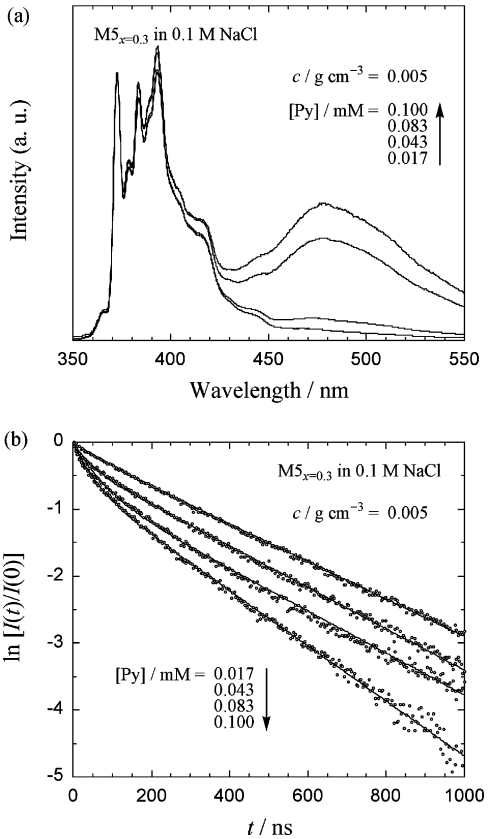

Figure 9. (a) Fluorescence spectrum of pyrene solubilized in 0.1 M aqueous NaCl solutions of sample $M5_{x=0.3}$ ($c = 5 \times 10^{-3}$ g/cm^3). (b) Decay of fluorescence around 400 nm for the solutions shown in panel a; curves in panel b, fitting results calculated by eqs 3 and 4.

Table 4. Parameters Obtained from the Fluorescence Decay Experiments for All Poly(NaAMPS/C_6MA) Samples

sample	$c/10^{-3}$ g cm^{-3}	C_{fast}/mM	[Py]/mM	$k_0/\mu s^{-1}$	$k_E/\mu s^{-1}$	$k_-/\mu s^{-1}$	$\bar{n}$	n_c
$M1_{x=0.3}$	7.1	0.12	0.045	2.7	9	1.0	0.45	0.83
	7.1	0.12	0.060	2.7	8	1.0	0.55	0.91
	7.1	0.12	0.089	2.7	7	1.1	0.68	1.1
$M2_{x=0.3}$	5.6	0.073	0.022	2.6	9	1.0	0.19	1.6
	5.6	0.073	0.086	2.6	7	1.0	0.72	1.6
	5.6	0.073	0.090	2.6	8	0.6	0.73	1.7
$M3_{x=0.3}$	5.1	0.022	0.027	2.5	6	0.26	0.26	4.7
$M5_{x=0.3}$	5.0	0.033	0.043	2.8	17	0.9	0.34	3.8
	5.0	0.033	0.083	2.8	15	1.5	0.6	4.1
	5.0	0.033	0.10	2.8	14	2.0	0.75	4.0
$M4_{x=0.2}$	9.6	0.13	0.025	3.0	17	0.24	0.19	1.0

Table 5. Hydrodynamic Radii Calculated by the Star Polymer Model Corresponding to the Small Aggregate (or the Fast-Relaxation Component) of the Poly(NaAMPS/C_6MA) Samples $M1_{x=0.3}$ and $M4_{x=0.2}$ in 0.1 M Aqueous NaCl

sample	n_c[a]	$m = N_{0w,fast}/N_{0w}$[a]	$R_{H,fast}$/nm	f[b]	$R_{H,linear}$/nm[c]	R_H/nm[d]
$M1_{x=0.3}$	1	5	4.6	5 (case 1)	5.0	4.4
				10 (case 2)	5.3	4.0
$M4_{x=0.2}$	1	2	6.8	2 (case 1)	6.2	6.2
				4 (case 2)	6.2	5.7

[a] Integer closest to the experimental result. [b] Number of arms of the star polymer model calculated by $f = m$ (case 1) or $2m$ (case 2). [c] Hydrodynamic radius of the linear polymer with the same degree of polymerization and intersegmental interaction. [d] Hydrodynamic radius of the star polymer model calculated by eqs 5 and 6.

excited pyrene molecule can form excimer with a ground-state one within its lifetime as detected by the strong fluorescence peak around 480 nm in Figure 9a.

Figure 9b shows the decay profiles of the fluorescence intensity $I(t)$ around 400 nm from pyrene solubilized in 0.1 M aqueous NaCl of sample $M5_{x=0.3}$ after pyrene is excited by a 337 nm light pulse of negligible duration at $t = 0$. While $I(t)$ decays single-exponentially with the lifetime of excited pyrene monomer at a low pyrene concentration [Py] ($= 17\ \mu$M), it exhibits a component with a faster decay at higher [Py]. This faster decay corresponds to the quenching of fluorescence of pyrene monomer by excimer formation within a hydrophobic microdomain (cf. Figure 9a), which returns to the ground-state emitting light around 480 nm being out of experimental window.

These fluorescence decay profiles were analyzed on the basis of the Infelta−Tachiya kinetics (eqs 3 and 4). Thin solid curves shown in Figure 9b demonstrate satisfactory fits of eqs 3 and 4 to the experimental $I(t)$. Similar analyses were made also for other poly(NaAMPS/C_6MA) samples, and all parameters determined are listed in Table 4. The decay rate constant k_0 of excited pyrene is almost independent of [Py] and the poly(NaAMPS/C_6MA) samples, as expected. The rate constants k_E for the excimer formation and k_- for exit of pyrene from the microdomain are mostly independent of [Py] but vary with the poly(NaAMPS/C_6MA) samples nonsystematically. At present, we have no interpretation of the poly(NaAMPS/C_6MA) sample dependencies of k_E or k_-.

The average number $\bar{n}$ of pyrene molecules per microdomain increases with [Py] in Table 4. If the fast-relaxation component or the small aggregate of poly(NaAMPS/C_6MA) contains n_c microdomains, $\bar{n}$ is equal to [Py]/($n_c C_{fast}$) where C_{fast} is the molar concentration of the fast-relaxation component calculated by $1000cN_A/M_{w,fast}$ with approximating w_{fast} to be 1. As shown in the last column of Table 5, n_c estimated by the above equation increases with $M_{w,fast}$ and also x of poly(NaAMPS/C_6MA), as expected, and is independent of [Py]. The latter independence guarantees that solubilized pyrene does not change n_c of the aggregate.

Discussion

As described above, the light scattering measurements have demonstrated that poly(NaAMPS/C_6MA) exists predominantly as aggregates of small numbers m ($= 2-7$) of chains in 0.1 M aqueous NaCl. On the other hand, fluorescence spectroscopy indicates that the small aggregate possesses n_c ($= 1-5$) hydrophobic microdomain(s) probably consisting of n-hexyl groups of poly(NaAMPS/C_6MA). In addition to this, the aggregates take more compact conformations than poly(NaAMPS) in 0.1 M aqueous NaCl (cf. Figure 7). These results indicate that poly(NaAMPS/C_6MA) chains aggregate through the hydrophobic core(s) and exist as micelles with n_c core(s) in the aqueous salt solution.

If all n-hexyl groups in poly(NaAMPS/C_6MA) are included in the hydrophobic core(s), the micelle should have many small loops. The average contour length of the NaAMPS sequence in the random copolymer can be calculated by $\sum_{\lambda=0}^{\infty} l\lambda x(1-x)^{\lambda} = l(1-x)/x$ with the mole fraction $(1-x)$ and the contour length l of the NaAMPS monomer unit, and the loop size l_{loop} is at most the half of the average length. On the other hand, the volume V_{core} of one core formed by n-hexyl groups may be calculated by $\upsilon_{hex} x M_{w,fast}/\bar{M}_0 n_c$ with the molecular volume υ_{hex} of n-hexane and the average molar mass $\bar{M}_0$ of the poly(NaAMPS/C_6MA) monomer unit. Therefore, the diameter d_{mic} of the micelle unit with one core may be approximately estimated by $d_{mic} = 2[l_{loop}/2 + (3V_{core}/4\pi)^{1/3}]$. Assuming the wormlike touched-bead model of the bead diameter d_{mic} and the persistence length equal to d_{mic},[26] we have calculated R_H for the micelles of all poly(NaAMPS/C_6MA) samples, as shown in Figure 7 by filled circles (for $x \sim 0.3$) and a filled triangle (for $x \sim 0.2$). The calculated R_H values are much smaller than the experimental results (the unfilled symbols), demonstrating that not all the n-hexyl groups attaching to poly(NaAMPS/C_6MA) chains are included in the hydrophobic cores of the aggregate. This may be because the intrachain electrostatic repulsion and local stiffness prevent NaAMPS sequences in the copolymer from forming such small loops.

In general, the unicore or multicore micelle can be viewed as a branched polymer, and the hydrodynamic radius can be written by[27]

$$R_{H,fast} = g_H R_{H,linear} \tag{5}$$

Here, g_H is the g-factor with respect to the hydrodynamic radius and $R_{H,linear}$ is the hydrodynamic radius of the linear polymer

with the same degree of polymerization and intersegmental interaction as those of the branched polymer. Among branched polymers with various architecture, the star-shaped polymer has been studied most extensively, and its g_H is empirically expressed as[27]

$$g_H(\text{star}) = \frac{f^{1/4}}{[2-f+\sqrt{2}(f-1)]^{1/2}} \frac{1-0.068-0.0075(f-1)}{1-0.068} \quad (6)$$

in a good solvent, where f is the number of arms of the star polymer. Unfortunately, the corresponding (general) equation for other branch architecture is not available at present.

The small aggregates of the poly(NaAMPS/C_6MA) samples $M1_{x=0.3}$ and $M4_{x=0.2}$ with a single core (cf. Table 4) may be modeled as a star polymer if each chain does not form any loops in the aggregate. When *n*-hexyl groups near the end of each copolymer chain are incorporated into the hydrophobic core, f of the star polymer is equal to the aggregation number m ($= M_{w,fast}/M_w$) of the small aggregates (case 1). On the other hand, when the core consists of *n*-hexyl groups in the middle portion of each copolymer chain, f is the twice of m (case 2). Thus, we may calculate $R_{H,fast}$ for those samples by eqs 5 and 6 in the case 1 or 2, if we have $R_{H,linear}$ of the reference linear polymer. (In a more general case where *n*-hexyl groups at arbitrary position of each copolymer chain are incorporated into the hydrophobic core, we can expect that R_H is between those of cases 1 and 2.) As mentioned above, however, since all *n*-hexyl groups are not incorporated into the hydrophobic core in the aggregates, the hydrophobic interaction acts among chains or arms in 0.1 M aqueous NaCl so that we cannot use R_H data for the poly(NaAMPS) linear homopolymer (the solid curve in Figure 7) in the same solvent as $R_{H,linear}$.

The intersegmental interaction in the poly(NaAMPS/C_6MA) aggregate may be characterized by the second virial coefficient $A_{2,fast}$, if the aggregation number does not change with the polymer concentration. From the fluorescence experiment for pyrene solubilized in 0.1 M aqueous solution of poly(NaAMPS/C_6MA), we know that the hydrophobic core formed by the copolymer is stable even at the concentration as low as 10^{-4} g/cm^3, and its number n_c per the aggregate is essentially independent of the polymer concentration. Since the size of the hydrophobic core should depend on the geometry or the chemical structure of the amphiphilic molecule but not on its concentration, we can expect that the aggregation number in the aqueous poly(NaAMPS/C_6MA) solution does not essentially change in the concentration range examined by the light scattering experiment.

In such a case, $A_{2,fast}$ may be expressed as[28]

$$A_{2,fast} = g_A(M_0/\bar{M}_0)^2 A_{2,linear} \quad (7)$$

where g_A is the *g*-factor with respect to A_2, and $A_{2,linear}$ is A_2 of the reference linear polymer with the same degree of polymerization and intersegmental interaction as those of the branched polymer (M_0: the monomer unit molar mass of the reference linear polymer). The *g*-factor g_A for star polymers in good solvents was experimentally estimated by several workers.[27] The results can be approximately expressed by the empirical equation $g_A(\text{star}) = 1 - 0.040(f-2)$. We can expect that the intersegmental interaction within the small aggregate of poly(NaAMPS/C_6MA) in 0.1 M aqueous NaCl is identical with that between poly(NaAMPS) linear homopolymer chains in the solvent where the right-hand side value of eq 7 is equal to $A_{2,fast}$ of poly(NaAMPS/C_6MA) in 0.1 M aqueous NaCl. Therefore, R_H data for poly(NaAMPS) in that solvent must be used as $R_{H,linear}$ in eq 5.

Fisher et al.[29] reported the degree of polymerization dependencies of A_2 and also $[\eta]$ of linear poly(NaAMPS) in aqueous NaCl solutions over the wide salt concentration range from 0.01 to 5 M. The comparison of their A_2 and our $A_{2,fast}$ data in the procedure above-mentioned indicated that the intersegmental interaction for the aggregate of sample $M1_{x=0.3}$ in 0.1 M aqueous NaCl is close to that of poly(NaAMPS) in 5 M (1 M) aqueous NaCl in case 1 (case 2), while that for the aggregate of sample $M4_{x=0.2}$ in 0.1 M aqueous NaCl is approximately equal to that of the homopolymer in 0.5 M in both cases 1 and 2. Thus, we should use R_H for poly(NaAMPS) under those corresponding solvent conditions as $R_{H,linear}$ in eq 5. Those values may be estimated by $(3[\eta]M_W/4\pi N_A\varphi)^{1/3}$ using the Mark−Houwink−Sakurada equations of Fisher et al. over the wide range of the NaCl concentration.

Table 5 lists $R_{H,linear}$ estimated in such a way and R_H for the star polymer model calculated by eqs 5 and 6. For both samples $M1_{x=0.3}$ and $M4_{x=0.2}$, R_H for the star polymer model of case 1 is close to $R_{H,fast}$ for the unicore micellar aggregates formed in 0.1 M aqueous NaCl. If the unicore micelles have loops, R_H must be reduced from that of the star polymer model of case 1. Thus, Table 5 indicates that the unicore micelles formed by both samples $M1_{x=0.3}$ and $M4_{x=0.2}$ do not take branching architecture with loops in 0.1 M aqueous NaCl.

Since general expressions for g_H and g_A are not available at present other than for the star polymer, it is not possible to make similar structural analyses for multicore micelles formed by samples $M2_{x=0.3}$, $M3_{x=0.3}$, and $M5_{x=0.3}$. However, for the aggregate formed by the highest molecular weight sample $M5_{x=0.3}$, n_c ($= 4$; cf. Table 4) is larger than m ($= 3$; cf. Table 2), so that we may expect at least two loops for the aggregate. As mentioned above, the formation of the loop may need sufficient chain length because of the electrostatic repulsion and chain stiffness. We can say that the chain length of sample $M5_{x=0.3}$ fulfills this requirement.

Since only few hydrophobic *n*-hexyl chains of each chain may be incorporated into the hydrophobic core, the "aggregation number" of *n*-hexyl chains per core is likely to be of the order of 10 for the aggregate of sample $M1_{x=0.3}$ and less for the aggregate of sample $M4_{x=0.2}$. These numbers are 1 order magnitude smaller than the aggregation number of the SDS micelle in aqueous salt solutions[30] but of the same order as that of sodium *n*-hexyl sulfate micelle recently reported.[31] The small aggregation numbers of *n*-hexyl chains indicate that the hydrophobic microdomain of poly(NaAMPS/C_6MA) is much different from the spherical micelle form by SDS, though the ratio I_3/I_1 of the solubilized pyrene in the microdomain is close to that in the SDS micelle (see above).

As reported by Strauss et al.,[32,33] viscosities of aqueous solutions of amphiphilic polyelectrolytes (i.e., polysoap) are dependent on the type and concentration of hydrophobic compounds solubilized in the aqueous solutions. Thus, the pyrene molecules solubilized for fluorescence experiments may cause some change in the structure of aggregates. To clarify this point, we measured viscosities for aqueous solutions of $M5_{x=0.3}$ to determine $[\eta]$. The $[\eta]$ value determined in the presence of pyrene was smaller by ca. 5% than that in the absence of pyrene, indicating that solubilization of pyrene molecules makes the size of aggregate smaller slightly. However, the time-resolved fluorescence data demonstrated that the number of cores was virtually constant independent of [Py] in

the whole [Py] region examined (Table 4). These observations indicate that the branched architecture of our copolymer aggregates is independent of whether pyrene molecules are solubilized, but the aggregation number of *n*-hexyl groups in each core slightly increases with increasing the solubilized pyrene concentration.

Concluding Remarks

We have estimated in this study the polymer aggregation number m and the number of hydrophobic cores n_c and discussed the possible branched architecture of the major small aggregates formed from statistical amphiphilic copolymers of NaAMPS and C_6MA in aqueous salt solutions. Those characteristics of the aggregates showed strong but somewhat peculiar dependencies on the degree of polymerization of the copolymer samples.

It is known that the comonomer sequence distribution may be a structural factor determining the architecture of aggregates formed from amphiphilic polyelectrolytes.[1] In the RAFT copolymerization of NaAMPS and C_6MA, a separate experiment on kinetics of RAFT copolymerization indicated that the rate of consumption for C_6MA was slightly faster than that for NaAMPS, indicating that poly(NaAMPS/C_6MA) may have parts rich with block sequences of C_6MA.[34] However, since RAFT copolymerization may yield polymer chains bearing practically the same distributions of comonomer sequence, we may not expect much different sequence distributions among our copolymer samples used in this study.

Acknowledgment. We are grateful to Professor Y. Morishima at Fukui University of Technology for fruitful discussion and valuable comments and also to Shoko Co., Ltd., for measuring SEC-MALS. This work was partly supported by a Grant-in-Aid for Scientific Research No. 17350058 from the Japan Society for the Promotion of Science.

Supporting Information Available: Preparation of 1-cyano-1-methylethyl dithiobenzoate (CMEDTB). This material is available free of charge via the Internet at http://pubs.acs.org.

References and Notes

(1) Hashidzume, A.; Morishima, Y.; Szczubialka, K. In *Handbook of Polyelectrolytes and Their Applications*; Tipathy, S. K., Kumar, J., Nalwa, H., Eds.; American Scientific Publishers: Stevenson Ranch, CA, 2002; Vol. 2, pp 1−63.
(2) Halperin, A. In *Supramolecular Polymers*; Ciferri, A., Ed.; Marcel Dekker: New York, 2000.
(3) Khougaz, K.; Astafieva, I.; Eisenberg, A. *Macromolecules* **1995**, *28*, 7135−7147.
(4) Zhang, L.; Eisenberg, A. *Science* **1995**, *268*, 1728−1731.
(5) Luo, L.; Eisenberg, A. *J. Am. Chem. Soc.* **2001**, *123*, 1012−1013.
(6) Burke, S. E.; Eisenberg, A. *Langmuir* **2001**, *17*, 6705−6714.
(7) Noda, T.; Morishima, Y. *Macromolecules* **1999**, *32*, 4631−4640.
(8) Chiefari, J.; Chong, Y. K.; Ercole, F.; Krstina, J.; Jeffery, J.; Le, T. P. T.; Mayadunne, R. T. A.; Meijs, G. F.; Moad, C. L.; Moad, G.; Rizzardo, E.; Thang, S. H. *Macromolecules* **1998**, *31*, 5559−5562.
(9) Chong, Y. K.; Le, T. P. T.; Moad, G.; Rizzardo, E.; Thang, S. H. *Macromolecules* **1999**, *32*, 2071−2074.
(10) Hawthorne, D. G.; Moad, G.; Rizzardo, E.; Thang, S. H. *Macromolecules* **1999**, *32*, 5457−5459.
(11) Kanao, M.; Matsuda, Y.; Sato, T. *Macromolecules* **2003**, *36*, 2093-2102.
(12) Tachiya, M. In *Kinetics of Nonhomogeneous Processes*; Freeman, G. R., Ed.; John Wiley & Sons: New York, 1987; pp 575−650.
(13) Thang, S. H.; Chong, Y. K.; Mayadunne, R. T. A.; Moad, G.; Rizzardo, E. *Tetrahedron Lett.* **1999**, *40*, 2435−2438.
(14) The specific refractive index increment ($\partial n/\partial c$) of dialyzed 0.1 M aqueous NaCl solution of NaAMPS homopolymer was determined to be 0.145 cm^3/g,[20] and using the result of ($\partial n/\partial c$) for M5$_{x=0.3}$ (0.147 cm^3/g; see Experimental Section), ($\partial n/\partial c$) for C_6MA homopolymer was estimated to be 0.154 cm^3/g. These ($\partial n/\partial c$) values indicate that the correction factor[35] to eqs 1 and 2 is very close to unity. Furthermore, $\langle S^2\rangle_{z,i}$ estimated by eq 2 is accurate enough, for random copolymers.[35]
(15) Infelta, P. P.; Gratzel, M.; Thomas, K. J. *J. Phys. Chem.* **1974**, *78*, 190−195.
(16) Infelta, P. P. *Chem. Phys. Lett.* **1979**, *61*, 88−91.
(17) Atik, S. S.; Nam, M.; Singer, L. A. *Chem. Phys. Lett.* **1979**, *67*, 75−80.
(18) Tachiya, M. *Chem. Phys. Lett.* **1975**, *33*, 289−292.
(19) Hagino, R.; Yashiro, J.; Norisuye, T., private communication.
(20) Yashiro, J.; Norisuye, T., private communication.
(21) From the concentration dependencies of $(Kc/R_\theta)_{fast}$ and Γ_{fast}/k^2, we examined the concentration dependence of the frictional coefficient for the small aggregate. The obtained concentration dependence was normal along with A_2 for all the samples, indicating that the small aggregates may be stable within the concentration range examined.
(22) Hagino et al.'s data[19] for [η] in 0.1 M aqueous NaCl obey the following Mark−Houwink−Sakurada equation at $M_w > 3 \times 10^4$: $[\eta] = KM_w^a$ with $K = 1.87 \times 10^{-3}$ cm^3/g and $a = 0.88$. Fisher et al.[29] reported the identical exponent a but a slightly smaller K for the same system.
(23) Tanford, C. *Physical Chemistry of Macromolecules;* John Wiley & Sons: New York, 1961.
(24) Kalyanasundaram, K.; Thomas, J. K. *J. Am. Chem. Soc.* **1977**, *99*, 2039−2043.
(25) Lianos, P.; Zana, R. *J. Phys. Chem.* **1980**, *84*, 3339−3341.
(26) Yamakawa, H. *Helical Wormlike Chains in Polymer Solutions;* Springer-Verlag: Berlin, 1997.
(27) Douglas, J. F.; Roovers, J.; Freed, K. F. *Macromolecules* **1990**, *23*, 4168−4180.
(28) Yamakawa, H. *Modern Theory of Polymer Solutions;* Harper & Row: New York, 1971.
(29) Fisher, L. W.; Sochor, A. R.; Tan, J. S. *Macromolecules* **1977**, *10*, 949−954.
(30) Lianos, P.; Zana, R. *J. Colloid Interface Sci.* **1980**, *84*, 100−107.
(31) Ruso, J. M.; Attwood, D.; Taboada, P.; Mosquera, V.; Sarmiento, F. *Langmuir* **2000**, *16*, 1620−1625.
(32) Strauss, U. P.; Assony, S. J.; Jackson, E. G.; Layton, L. H. *J. Polym. Sci.* **1952**, *9*, 509−518.
(33) Strauss, U. P.; Gershfeld, N. L. *J. Phys. Chem.* **1954**, *58*, 747−753.
(34) Hashidzume, A.; Hyoda, K.; Kawaguchi, A.; Morishima, Y., unpublished work.
(35) Benoit, H.; Froelich, D. In *Light Scattering from Polymer Solutions*; Huglin, M. B., Ed.; Academic Press: London, 1972; Vol. 27, pp 467−501.

MA051950D